A Computational Framework for Particle and Whole Cell Tracking Applied to a Real Biological Dataset

F. Yang[1], C. Venkataraman[2], V. Styles[1], V. Kuttenberger[3], E. Horn[3], Z. von Guttenberg[3] and A. Madzvamuse[1]

1. University of Sussex, UK, 2. University of St Andrews, UK, 3. ibidi GmbH, Germany

University of Sussex

Introduction

Cell tracking is becoming increasingly important in cell biology as it provides a valuable tool for analysing experimental data and hence furthering our understanding of dynamic cellular phenomena. The advent of high-throughput, high-resolution microscopy and imaging techniques means that a wealth of large data is routinely generated in many laboratories. The development of computer algorithms for automated cell tracking is thus highly desirable.

In this work, we describe two approaches to automated cell tracking in two different scales: segmentation followed by particle tracking and the problem of whole cell tracking in which one wishes to reconstruct in time whole cell morphologies.

Cell Culture and Microscopy

The human fibrosarcoma cell line HT-1080 (obtained from DSMZ, Germany) was grown in Dulbecco's modified Eagle's Medium (DMEM, Sigma-Aldrich) supplemented with 10% fetal bovine serum (FBS, Sigma-Aldrich) at $37°C$ and 5% CO_2. To perform a migration experiment without chemoattractant both reservoirs and the channel were filled with DMEM with 5% FBS. The time-lapse interval was ten minutes over a time period of 24 hours.

Cell Tracking by Detection

The first step is to individually represent each cell by a single dot (typically the centre of the mass), this is achieved using segmentation. The second step is to determine the correspondences of cells from one frame to the other.

Phase-contrast Microscopy Images

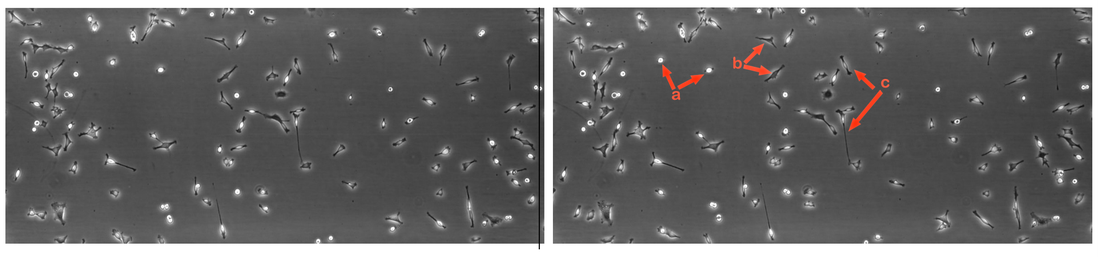

In the above figure, two typical phase-contrast microscopy images (the first and second frames on the left and right, respectively) from ibidi GmbH are illustrated.

(a) cell nuclei have been marked with phase-contrast with little halo artefacts;

(b) the fluorescent is obscured but leaves a halo artefact around the edges of the cell membrane;

(c) various intensities of phase-contrast from the nuclei and elongated cells.

Segmentation

We introduce some straightforward but very effective segmentation techniques, namely the background subtraction [3] (see the left-hand side figure below) and standard image enhance techniques (see the right-hand side figure below). We mark each identified cells with a red circle.

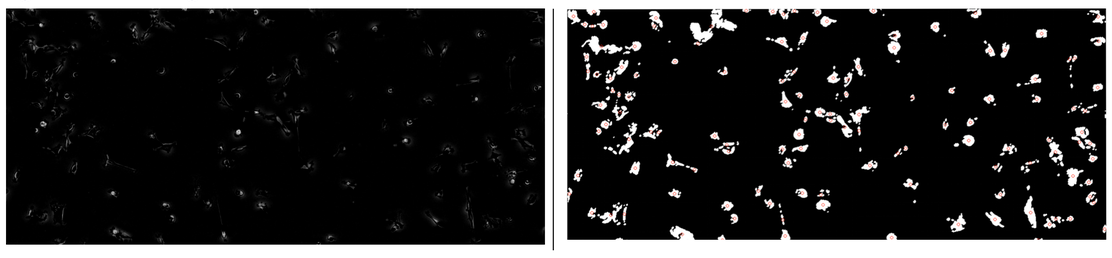

Particle Tracking

The particle tracking method we follow is a straightforward nearest-neighbour approach where particles between frames are linked to their nearest neighbours. Our algorithm gives 61 persistent cells and comparing against 63 persistent cells from using manual-tracking.

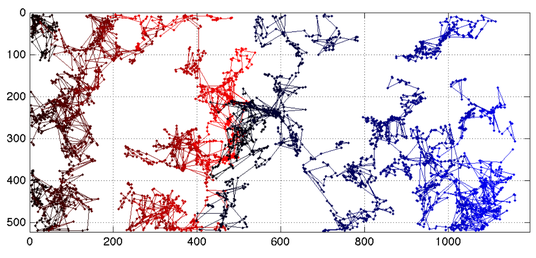

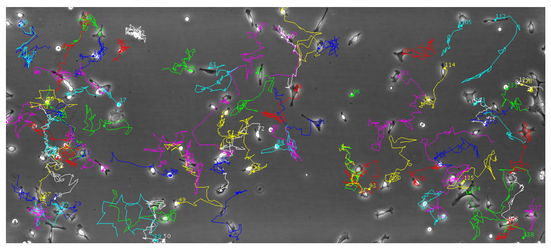

Data Analysis

We observe no clear directional bias which is as expected: the dataset is without a chemoattractant.

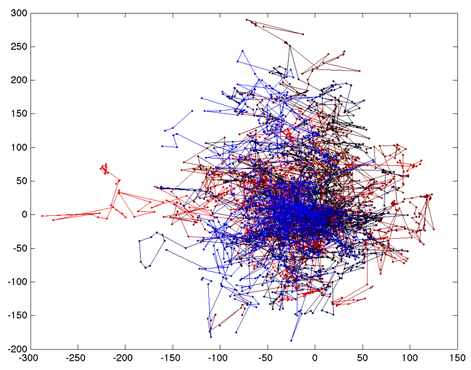

Acknowledgements

We acknowledge the support from the following funding bodies.

Isaac Newton Institute for Mathematical Sciences

The Leverhulme Trust

Whole Cell Tracking

In this section we broaden the focus from tracking cell centroids to tracking whole cell morphologies with the goal of recovering morphological dynamics. The aim is to determine trajectories of points on the cell boundary from position A at time 0 to position B observed at time T.

Mathematical Model

We consider the mass constrained Allen-Cahn equation with forcing,

$$\begin{cases} \epsilon\frac{\partial}{\partial t}\phi(\vec{x},t) = \epsilon\triangle\phi(\vec{x},t) - \epsilon^{-1}G'(\phi(\vec{x},t)) + \eta(\vec{x},t) + \lambda(t) & in\ \ \Omega\times(0,T], \\ \phi(\vec{x},0) = \phi^0(\vec{x}) & in\ \ \Omega, \\ \nabla\phi(\vec{x},t)\cdot\vec{\nu}_\Omega(\vec{x}) = 0 & on\ \ \partial\Omega, \end{cases} \tag{1}$$

where $\phi(\vec{x},t)$ is a phase-field variable, $\epsilon > 0$ governs the interfacial width, $G(\phi) = \frac{1}{4}(1-\phi^2)^2$ is a double well potential, λ is a mass constraint [2] and $\vec{\nu}_\Omega$ is the normal to $\partial\Omega$. We introduce the objective functional J, which we seek to minimise

$$J(\phi,\eta) = \frac{1}{2}\int_\Omega (\phi(\vec{x},T) - \phi_{obs}(\vec{x}))^2\, d\vec{x} + \frac{\theta}{2}\int_0^T\int_\Omega \eta^2(\vec{x},t)d\vec{x}dt, \tag{2}$$

where $\theta > 0$ is a regularisation parameter. On the right-hand side of (2), the first is the so called fidelity term and the second term is the regularisation.

Given initial data ϕ^0 and target dataset ϕ_{obs}, find a space-time distributed forcing $\eta^* : \Omega\times[0,T) \to \mathcal{R}$ such that with ϕ a solution of (1) with initial condition $\phi(\cdot,0) = \phi^0(\cdot)$, the forcing η^* solves the minimisation problem

$$\min_\eta J(\phi,\eta), \quad with\ \ J\ \ given\ \ by\ \ (2). \tag{3}$$

Morphological and Movement Reconstruction

We select two cells with their initial states (shapes in the first frame), their desired states (shapes in the second frame) and include their phase-field representations.

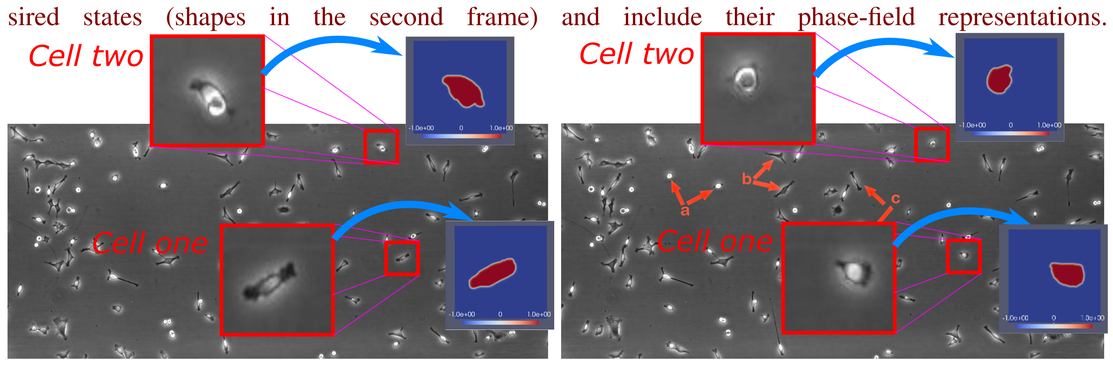

The reconstructed morphologies are displayed below where we present the initial states, shapes at halfway mark and the computed final time. We also include the forcing η at the zero-isosurface in the second row.

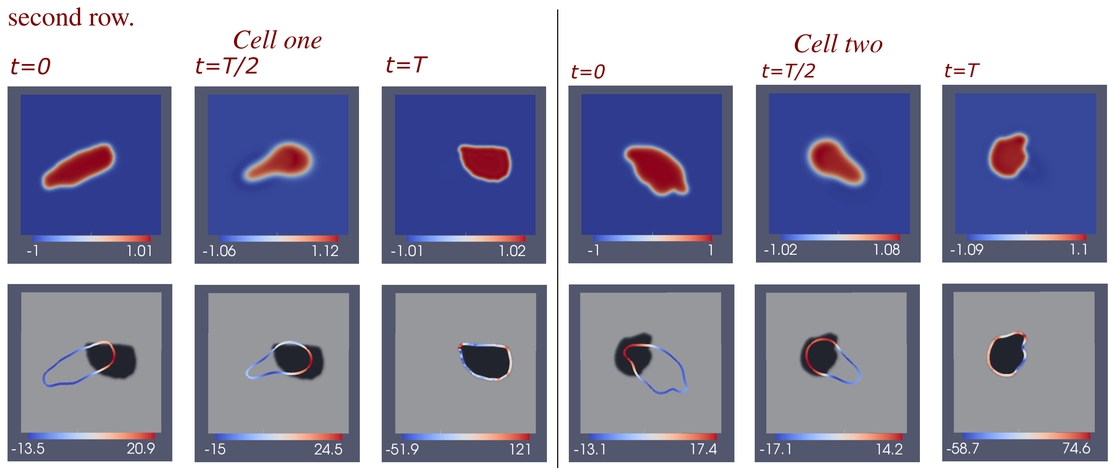

Data Analysis

We illustrate the changes in mass and volume. The linear interpolations of mass are intended by our mass-constraint [1,2].

Mass ($\int_\Omega \phi d\vec{x}$)

Volume ($\int_{\{\phi>0\}} 1 d\vec{x}$)

References

1. F.W. Yang *et al. A robust and efficient adaptive multigrid solver for the optimal control of phase-field formulations of geometric evolution laws*, under review, 2015.
2. K.N. Blazakis *et al. Whole cell tracking through the optimal control of geometric evolution laws*, Journal of Computational Physics, 2015.
3. M. Xian *et al. A background reconstruction algorithm based on intensity extremum classification*, Advances in Information Sciences and Service Sciences, 2012.